








Two-dimensional peripheral refraction in adults

XIAOYUN XI,¹  JIANGDONG HAO,¹ ZHENGHUA LIN,²  SIDI WANG,^{1,3}  ZHIKUAN YANG,^{1,4} WEIZHONG LAN,^{1,4,5}  AND PABLO ARTAL^{1,6,*} 

¹Aier School of Ophthalmology, Central South University, Changsha, China

²Aier Institute of Optometry and Vision Science, Aier Eye Hospital Group, Changsha, China

³Shaanxi Eye Hospital, Xi'an People's Hospital (Xi'an Fourth Hospital), China

⁴School of Stomatology and Ophthalmology, Xianning Medical College, Hubei University of Science and Technology, China

⁵Guangzhou Aier Eye Hospital, Guangzhou, China

⁶Laboratorio de Óptica, Universidad de Murcia, Campus de Espinardo, Murcia, Spain

*pablo@um.es

Abstract: Peripheral refraction has been studied for decades; however, its detection and description are somehow simplistic and limited. Therefore, their role in visual function and refractive correction, as well as myopia control, is not completely understood. This study aims to establish a database of two-dimensional (2D) peripheral refraction profiles in adults and explore the features for different central refraction values. A group of 479 adult subjects were recruited. Using an open-view Hartmann–Shack scanning wavefront sensor, their right naked eyes were measured. The overall features of the relative peripheral refraction maps showed myopic defocus, slight myopic defocus, and hyperopic defocus in the hyperopic and emmetropic groups, in the mild myopic group, and in other myopic groups, respectively. Defocus deviations with central refraction vary in different regions. The defocus asymmetry between the upper and lower retinas within 16° increased with the increase of central myopia. By characterizing the variation of peripheral defocus with central myopia, these results provide rich information for possible individual corrections and lens design.

© 2023 Optica Publishing Group under the terms of the [Optica Open Access Publishing Agreement](#)

1. Introduction

Peripheral defocus plays an important role in peripheral vision and potentially in the eyeball development. First, peripheral vision is important in mobility and precision for some sports [1] and tasks [2–5]. Second, peripheral vision provides the only visual information for patients suffering from macular diseases, such as macular hole and age-related macular degeneration [6]. Peripheral defocus also affects eye development and myopia progression [7,8]. Furthermore, animal studies involving chicks [9] and monkeys [10,11] have shown that the mechanism of the regulation of eye development and experimental myopia is locally controlled by the retina. In clinical applications, lenses designed to impose myopia defocus in the periphery also exhibit some effects to reduce myopia development [12–15]. Studies [16–18] concerning the impact of refractive blur on peripheral vision using different stimuli have found that detection acuity varies strongly with defocus; in other words, defocus is the most relevant optical factor, in addition to astigmatism, higher-order aberrations, and scattering, affecting peripheral vision.

At present, refractive corrections are focused exclusively on central vision, with minimal concerns about their possible effects in peripheral vision. Some special lenses designed to control myopia progression induce peripheral defocus that is uniform, with a magnitude obtained from average data [19,20] rather than from individual values. However, the peripheral refraction distribution of each person is different; thus, currently applied lenses are not accurately inducing the desired peripheral refraction. Consequently, myopia prevention and control results for

different individuals using the same lens are also considerably different. To accurately correct peripheral refraction and induce a precise amount of defocus in the periphery, we should first obtain precise data on peripheral refraction distribution.

The interest in peripheral refraction lasted for 90 years since Ferree et al. tested it with a coincidence optometer in 1931 [21]. Most research has suggested that myopic eyes usually have a relative hyperopic defocus in the periphery; in contrast, hyperopic eyes are usually myopic in the periphery relative to the center [22–27]. However, given the lack of accuracy and precision of the equipment or inefficient operations, the regional profile [24] has only been described by a number of papers, and no clear and agreed results [23–25] for the symmetry patterns of peripheral defocus in the retina have been established.

Jaeken et al. [28] developed an instrument based on Hartmann–Shack (H-S) technology, which has greatly improved detection efficiency. With this instrument, Lan et al. [29] studied peripheral refraction and retinal image quality in emmetropic children, and Wang et al. [30] compared the refraction of adults with isomyopia and anisomyopia. However, these studies had fewer subjects and limited refraction groups. In this study, groups of hyperopes, emmetropes and myopes subjects were included to further study the two-dimensional (2D) features of peripheral defocus in adults.

2. Methods

2.1. Participants

A group of 479 Asian adults was recruited from Xiangya Medical College. This study was approved by the Committee of Research Ethics of the Aier School of Ophthalmology, Central South University (ID: AIER 20191RB16) and conducted in accordance with the tenet of the Declaration of Helsinki. Each participant signed an informed consent form after a detailed explanation of the procedures and risks involved.

The inclusion criteria were: (1) The best corrected visual acuity of 20/20 or better in the right eye, (2) was free of ocular diseases, (3) no previous ocular surgery, (4) no amblyopia or strabismus, (5) no lens changes or opacities, and (6) had not worn any orthokeratology for at least 3 months (7) no history of wearing any other myopia control lenses. The preliminary examinations for the inclusion criteria included evaluating general health, best-corrected visual acuity, and direct ophthalmoscope detection.

The group consisted of 134 males and 345 females, with an average age of 24.87 ± 5.33 years, ranging from 17–50 years; the average central refraction was -4.69 ± 2.86 D, ranging from -10.64 D to 4.14 D. The details of the participants, such as gender, age, and spherical equivalent (SE) refraction, in different groups are shown in Table 1. No statistically significant difference was found between the genders (mean central spherical equivalence values in females and males were -4.53 ± 2.93 D and -4.76 ± 2.84 D; $F = 0.383$, $P = 0.43$).

Table 1. Demographic information of participants ($n = 479$, M \pm SD)^a

	(+0.5, 5] D	(-0.5, +0.5] D	(-2, -0.5] D	(-4, -2] D	(-6, -4] D	(-12, -6] D
Female	5	12	63	55	74	136
Male	1	14	20	26	23	50
Total	6	26	83	81	97	186
Age (y)	30.7 \pm 8.91	29.5 \pm 6.87	27.2 \pm 6.66	25.0 \pm 4.30	24.4 \pm 4.92	23.2 \pm 3.89
CSE (D)	1.85 \pm 1.548	-0.23 \pm 0.208	-1.24 \pm 0.459	-3.00 \pm 0.574	-5.02 \pm 0.607	-7.63 \pm 1.059

^aM = mean; SD = standard deviation; CSE = central spherical equivalent; y = years old; D = diopter

2.2. Instrumentation and data collection

Peripheral refraction was measured in the right eyes of each subject using an open-view H-S wavefront sensor (Voptica peripheral refractor [29], Voptica SL, Murcia, Spain), which was previously described in detail [29,30]. The naked eyes of each subject were measured after staying in a darkroom for 30 minutes. The details of the VPR measuring process were also previously described [30]. We computed the power vector components of the eye's spherical refractive error M using the following equations from second-order Zernike terms. Where C is the Zernike coefficient for defocus, and r is the pupil radius (4 mm was performed in this study).

$$M = -\frac{4\sqrt{3}}{r^2}C_2^0 \text{ (diopter)}$$

2.3. Data analysis and statistics

The subjects were classified into six groups according to their central spherical equivalent (CSE) to investigate the relative peripheral refraction (RPR) for each refractive group: (1) G1: (+0.5, 5] D; (2) G2: (-0.5, +0.5] D; (3) G3: (-2, -0.5] D; (4) G4: (-4, -2] D; (5) G5: (-6, -4] D; and (6) G6: (-12, -6] D. Each 2D-RPR map was divided into nine (3×3) sections or four rings to investigate the local retinal behavior of the RPR. Data around the optic disk were excluded from analysis in the nine-grid zoning method (horizontal: nasal 13.5° to 21.5°, vertical: superior 5.5° to inferior 3.5°) and in the four-ring zoning method (circle center coordinates: x-coordinate: nasal 17.5° and y-coordinate: superior 1°, circle diameter: 4.5°). Figure 1 shows schematic representations of the different spatial analyses performed. **A)** The rectangular grid was set on vertical ±5.5° and horizontal ±10.5°. **B)** In four-ring zoning method, four annular regions with diameters of 16°, 12°, 8°, and 4° were set. **C)** For the asymmetry analysis, the circular map was divided into upper and lower parts according to horizontal lines, and the upper and lower areas were divided into three areas according to the ±45° line. The defocus of asymmetry index (DAI) of each subject is the absolute value of the difference between the values of symmetric points in the upper and lower retinas.

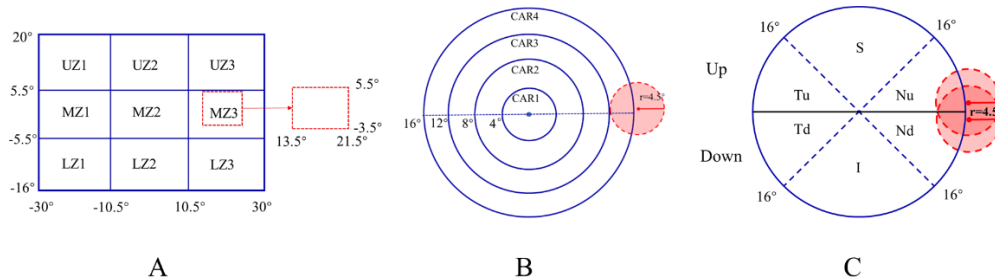


Fig. 1. Codes used for the different zones in the statistical analysis (see additional details in the text). The red dotted lines in picture A and the red circles in pictures B and C represent the optic disk areas that are not included in the analysis.

The 2D peripheral refraction maps of every single eye were calculated using MATLAB (MathWorks Inc., Natick, MA, USA). The original data of all 2D maps were derived from 10 horizontal sections corresponding to 610 (61 × 10) SE values across the retina. For each map, the x-axis value from the negative to the positive position presents the horizontal positions from the temporal to the nasal retina, and the y-axis value from the negative to the positive position presents the vertical positions from the inferior to the superior retina. SPSS software (IBM SPSS Statistics 25) was used for the statistical analysis. A one-way ANOVA was used to compare the age and CSE in different groups, the average refractions in different areas within the groups, the

average refractions of the corresponding sections in different groups, and the average DAI in different groups. A paired t-test was used to compare the RPR asymmetry values of the up and down retinas obtained by two symmetric analysis methods within groups. Regression analysis was used to determine the shifting characteristics of the different regions. Two-tailed $p < 0.05$ was set as a statistically significant level.

3. Results

3.1. Comparison of local average RPR within refractive groups

In order to clarify the characteristics of peripheral refraction in each group, we divided the map into eight peripheral and one central regions, and compared the mean value of each peripheral region with the central one. Figure 2 shows the 2D RPR maps for the six groups and comparisons between the peripheral regions and the central region MZ2 within every group. The maps were obtained by subtracting the corresponding CSE from the original maps and then averaging the maps in the same group. We then calculated the average values of each zone for comparison with the M2 value, and the details of the regional average RPR values in every group are presented in Supplement 1. Astigmatism and higher order aberrations were also obtained. These results are presented as a Supplement 1.

In the (0.5, 5.0] D and (-0.5, 0.5] D groups, the relative peripheral defocus was myopic, which was small for the emmetropic subjects. In the (-2.0, -0.5] D group, the map was nearly flat, with regions MZ3 and UZ2 showing a slight hyperopic shift and some mild relative myopia, respectively. For the (-4.0, -2.0] D to (-12.0, -6.0] D groups, the nasal and temporal sides showed significant relative hyperopia that increased with the amount of central myopia. In these groups, however, the regions UZ2 and LZ2 exhibited a small difference from the center.

Scatter diagrams of the regression analysis of the RPR values as a function of CSE in each zone are presented in Fig. 3 and Table 2. The result shows that all regression lines are statistically significant, with $P < 0.000$. The slopes of different area regression lines were compared in sequence: UZ3 > UZ1 > MZ1 > LZ1 > MZ3 > LZ3 > UZ2 > MZ2 > LZ2. We noticed that the RPR in the upper retina changed the most in UZ3 and UZ1, followed by the temporal retinas MZ1 and LZ1, and then the nasal retinas MZ3 and LZ3. The slowest area was in the central retinas of UZ2, MZ2, and LZ2.

Table 2. Regression analysis results of the nine regions

	<i>R</i>	<i>R</i> Square	Adjusted <i>R</i> Square	Unstandardized Coefficients		Standardized Coefficients Beta	<i>t</i>	Sig.
				Constant	<i>B</i>			
UZ1	0.581	0.338	0.336	-0.247	-0.259	-0.581	-15.593	0.000
UZ2	0.463	0.214	0.213	-0.220	-0.120	-0.463	-11.405	0.000
UZ3	0.592	0.351	0.349	0.095	-0.268	-0.592	-16.051	0.000
MZ1	0.575	0.331	0.329	-0.067	-0.192	-0.575	-15.345	0.000
MZ2	0.261	0.068	0.066	0.080	-0.020	-0.261	-5.904	0.000
MZ3	0.545	0.297	0.295	0.226	-0.21	-0.545	-14.190	0.000
LZ1	0.546	0.299	0.297	0.038	-0.211	-0.546	-14.249	0.000
LZ2	0.241	0.058	0.056	-0.112	-0.041	-0.241	-5.425	0.000
LZ3	0.505	0.255	0.253	-0.166	-0.186	-0.505	-12.778	0.000

3.2. RPR in different eccentricities between and within groups

We compare the RPR of different eccentricity regions according to the four-ring zoning method in Fig. 1(B) to explore the RPR distribution along with eccentricities. Figure 4(A) shows the

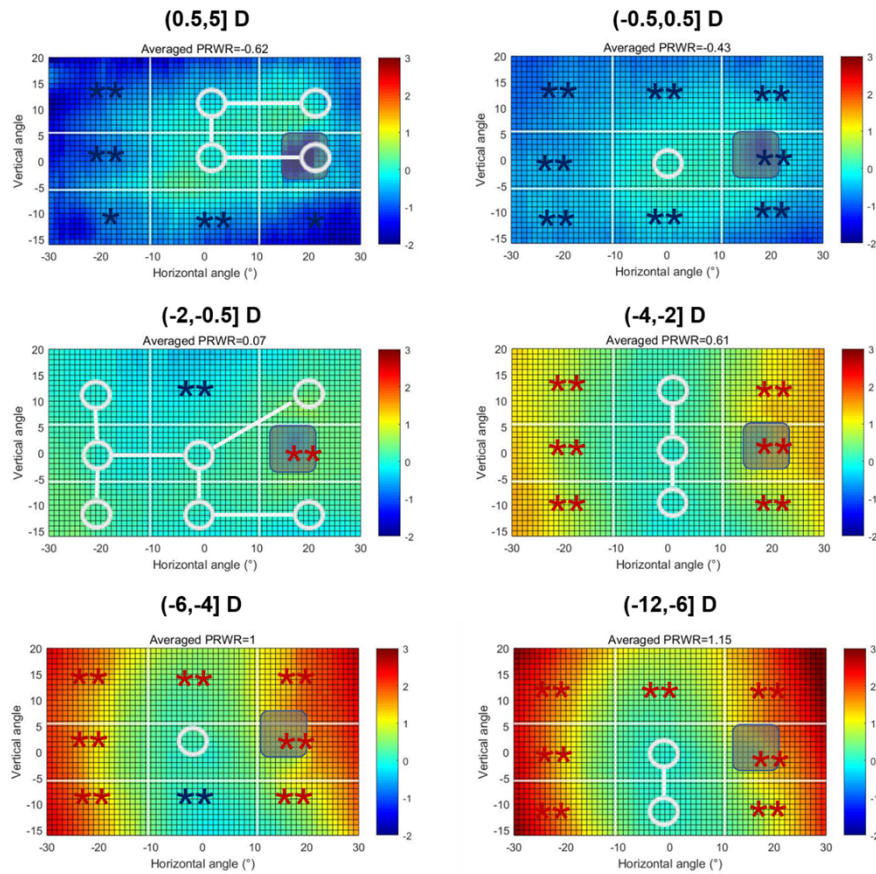


Fig. 2. Averaged two-dimensional (2D) maps of the relative peripheral refraction (RPR) in the six refractive groups. The positive and negative values on the x-axis indicate the nasal-retinal and temporal-retinal and for the y-axis, the positive and negative values represent the superior and inferior retinas, respectively. The color code is in diopters. The white circle represents no statistical difference between the zone and the center zone MZ2, and the blue star (*) or red star (*) presents a statistically myopic or hyperopic difference, respectively. The color code for each map was uniformly set, ranging from -2 D to 3 D.

evolution of the RPR for each group. CAR4 is the outmost region with the largest eccentricity from the 4-ring method, which can better reflect the defocus trend. Subjects in groups $(0.5, 5.0]$ D and $(-0.5, 0.5]$ D had a large myopic defocus with increasing eccentricity, with CAR4 values of -0.39 ± 0.45 D and -0.32 ± 0.27 D, respectively. In group $(-2.0, -0.5]$ D, the RPR remained near zero, with a CAR4 value of -0.018 ± 0.030 D. Subjects in groups $(-4.0, -2.0]$ D, $(-6.0, -4.0]$ D, and $(-12.0, -6.0]$ D present a hyperopic RPR that increases with eccentricity, with CAR4 values of -0.26 ± 0.36 D, -0.43 ± 0.40 D, and -0.52 ± 0.41 D, respectively. ANOVA analysis was performed to compare the RPR in the four rings within groups, and the results indicate a statistically significant difference in all groups except in groups $(-0.5, 0.5]$ D ($F = 2.514$, $P = 0.088$) and $(-2.0, -0.5]$ D ($F = 1.412$, $P = 0.239$); linear test results indicate that the RPR in the four rings are linearly related in all groups except in group $(-2.0, -0.5]$ D ($F = 1.004$, $P = 0.317$). The details are presented in [Supplement 1](#).

Figure 4(B) represents the peripheral defocus for each group and eccentricity. CAR1 changed from 0.032 ± 0.055 D in group $(0.5, 5.0]$ D to 0.063 ± 0.15 D in group $(-12.0, -6.0]$ D, with a

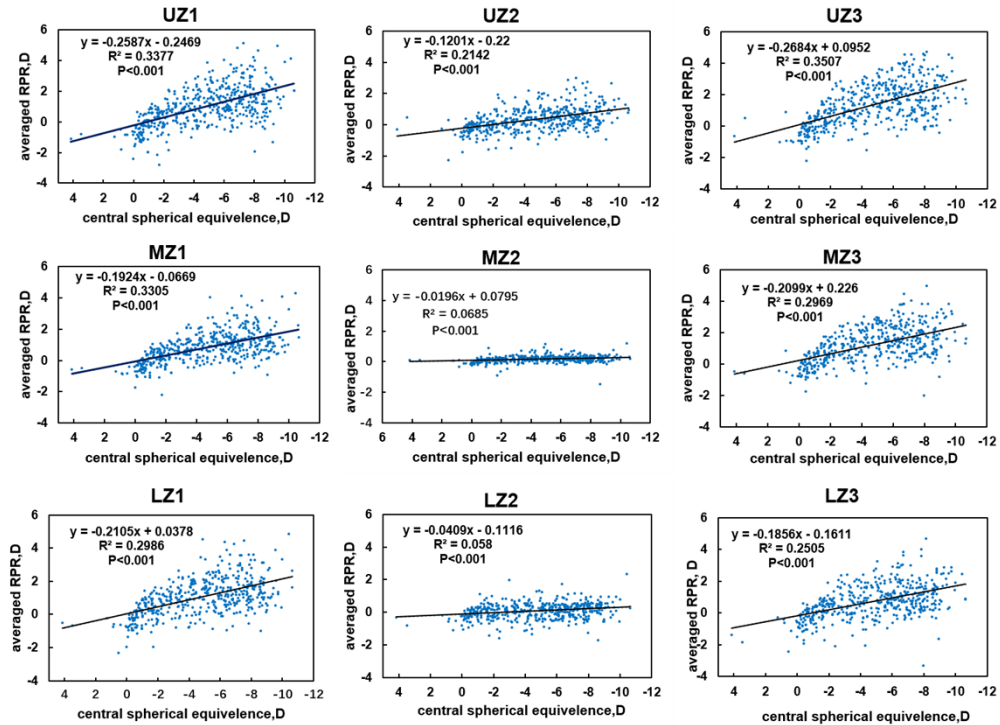


Fig. 3. Fitting curves of regional averaged relative peripheral refraction (RPR) along with central spherical equivalent (CSE) in nine zones. The x-axis indicates the CSE, whereas the y-axis presents the averaged RPR value of the zone. The regression equation is shown in the upper left corner.

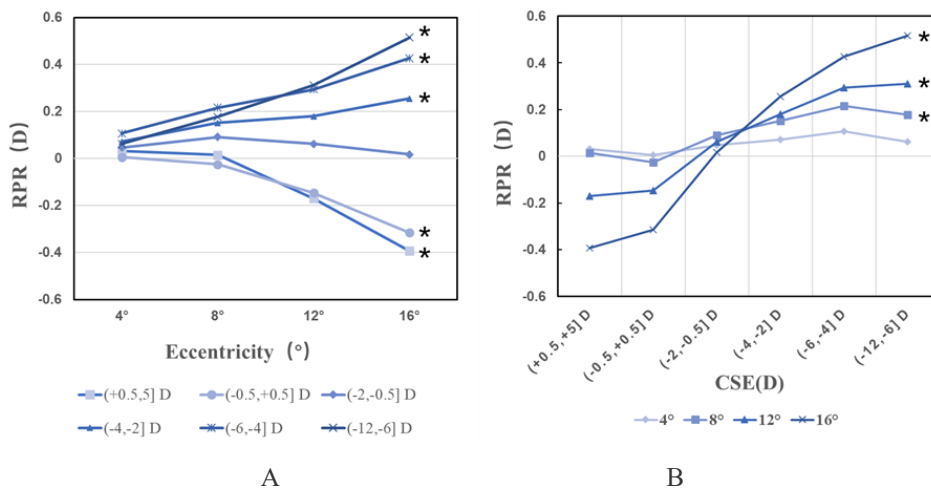


Fig. 4. Average relative peripheral refraction (RPR) in six groups of the four annular regions. In picture A, the x-axis shows rings with different eccentricity, and the y-axis in diopters shows the averaged refraction of the annular areas. In picture B, the x-axis shows the six groups, and the y-axis in diopters shows the averaged refraction of annular areas. The asterisks* represent statistical differences in linear test results in both Figs. (A) and (B).

difference value of 0.031 D; the same difference values in CAR2 and CAR3 were 0.16 D and 0.48 D, respectively, whereas CAR4 had a value of 0.91 D. The ANOVA results indicate a significant difference between the different groups at the annular areas ($P < 0.05$) and linear test results indicate that the RPR only in CAR1 represent no significant difference ($F = 2.460$, $P = 0.117$). The ANOVA results are shown in [Supplement 1](#).

3.3. Symmetry analysis

We calculated the X axis-symmetric index between the up and down semicircles, S and I, Tu and Td, and Nu and Nd and the centro-symmetric index between S and I. The DAI of each subject is the absolute value of the difference between symmetric points, axisymmetric points refer to two points that overlap after folding along the horizontal meridian, and centro-symmetric points refer to a pair of points that are symmetrical with the coordinate original (the fovea). The mean values in each group (except group (0.5, 5.0] D, which was eliminated because the population was too small) were calculated to make comparisons between different groups.

Figure 5 shows the axis-symmetric values of each group. The values increased with central myopia, with an S-I value larger than that of Tu-Td and Nu-Nd in each group. The up-down value changed from 0.29 ± 0.19 D in group (-0.5, +0.5] D to 0.51 ± 0.31 D in group (-12.0, -6.0] D; and the S-I value changed from 0.35 ± 0.29 D in group (-0.5, +0.5] D to 0.66 ± 0.49 D in group (-12.0, -6.0] D as the largest paired area. The numerical values are presented in [Supplement 1](#). The ANOVA analysis of DAI in up-down, S-I, Tu-Td, and Nu-Nd between groups indicates a statistical difference between groups and that the DAI values are linearly increasing significantly ($P < 0.001$).

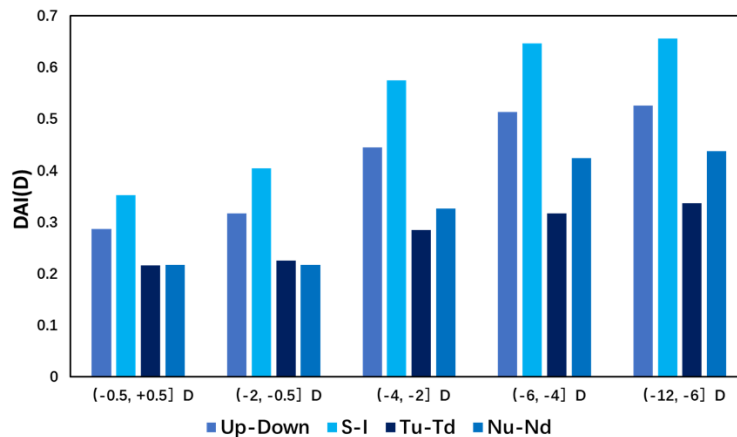


Fig. 5. Average axisymmetric values of the four symmetric regions (up-down, S-I, Tu-Td, and Nu-Nd) in the five groups. The x-axis shows the four symmetric regions in five groups, and the y-axis in diopters represents the averaged axisymmetric value.

3.4. X axis-symmetric and centro-symmetric DAI on S-I

To further understand the difference between the nasal and temporal sides, we calculated the DAI values between the superior and inferior retinas using axisymmetric and centrosymmetric methods. The results show a significant difference, with a minute difference in values ranging from 0.017 D to 0.054 D, indicating that the defocus is slightly asymmetric on the nasal and temporal retina. Figure 6 demonstrates the results of the axisymmetric and centrosymmetric DAI in the S-I area. The difference value between the axisymmetric DAI and centrosymmetric DAI was 0.017 D in group (-0.5,0.5] D, which was the smallest in all five groups, and 0.054 D in

group ($-6.0, -4.0$] D, which was the largest in all groups—all indicating a mere difference. A paired t-test was performed between the axisymmetric and centrosymmetric DAI in each group, and the result shows a significant difference in each group, with $P < 0.01$; however, none of them reached a clinical difference. Furthermore, two classes of DAI values both increased with the increase of central myopia degree, and the ANOVA linear analysis showed $P < 0.000$, both in the two series data. Detailed information is presented in [Supplement 1](#).

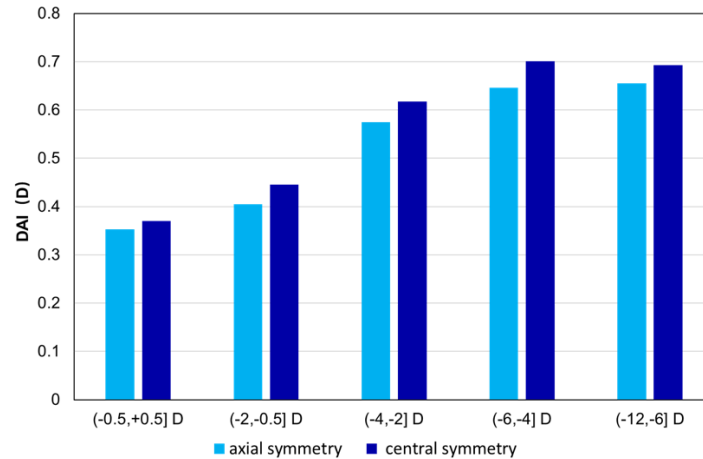


Fig. 6. Comparison of axisymmetric and centrosymmetric defocus asymmetry indices in the S-I area

4. Discussion

Cross-sectional research was conducted to obtain the 2D peripheral refraction patterns and associated features in adults and to explore their variation with central ametropia. We chose adults in this study for several reasons, first, myopia increases even in adulthood, so it is especially helpful for people who are interested in refractive surgery but fear further myopia after surgery; second, it helps us to understand the evolution of myopia from children to adults and the peripheral defocus' characteristics in myopia; third, it is helpful to understand the visual quality of adults compared with children. A total of 479 subjects were divided into six groups according to their central refraction (i.e., CSE). For each subject, a 2D map covering $60^\circ \times 36^\circ$ visual field was recorded for a high-resolution pupil diameter of 5 mm (every one degree). We divided the relative refraction maps into several sections using different approaches to better understand the local characteristics. Given that a previous study [30] has found that the RPR topographic maps in the left and right eyes are mirror symmetric, we measured the right eye only rather than measuring both eyes.

The results indicate that the hyperopes show peripheral relative myopic defocus, emmetropes present peripheral flat defocus, and myopes tend to have hyperopic defocus, which is consistent with previous studies [22–27,30]. The RPR distribution was associated with eccentricity, and the greater the eccentricity, the greater the absolute value of the RPR. Other studies have also previously shown a similar behavior [31–33]; however, these studies were restricted to some particular meridians and did not cover the entire area. In this study, the measurements covered an extended area of the retina using high-density sampling. We confirmed the idea that RPR shifts from myopia to hyperopia as central myopia increases, for the possible reasons as suggested by several previous studies [34–36] is principally attributed to the change of eyeball shape.

An important and novel contribution of this work is related to the spatial distribution of peripheral refraction. In the nine-grid division approach, RPR in the six groups is not uniform, and the nasal and temporal retinas show a considerable hyperopic shift, whereas the inferior retina shows a myopic shift, which is also consistent with our previous results. In addition, several other studies [34,37] have also shown that myopes have prolate-shaped eyes, with refractive errors tending to be relatively hyperopic in the peripheral refraction. The scatter diagrams in Fig. 3 show that the average defocus of each region varies with the center diopters. Among the slopes of the nine fitting curves, UZ1 and UZ3 in the upper retina reached 0.26 and 0.27, respectively, whereas the lower retina LZ2 was the smallest at 0.04. This result indicates that the shift in peripheral defocus in LZ2 is the slowest and most consistent with the central diopter. We may speculate that such changes are related to the shape of the eye; that is, with the increase of central myopia, the fovea in the posterior and lower parts of the retina grows more rapidly to the rear, whereas the upper part of the retina grows relatively slowly. However, peripheral defocus is affected by a variety of factors except eyeball shape such as thickness of retina and status of cornea and crystalline lens, specific mechanisms researches are still need in the further.

Through the annular partition of the topographic map within the 16° scope, we found that the RPR increased with eccentricity, including myopic defocus in hyperopes and hyperopic defocus in myopes, whereas in the low myopia group ($-2.0, -0.5$] D, the RPR was flat.

The result of the nine-grid division method shows that the defocus varies asymmetrically in different areas of the retina with different asymmetries; meanwhile, the annular partition method shows regularity with eccentricity. To clarify this asymmetric distribution of the RPR, we analyzed the asymmetry of the RPR in the up and down retinas within the 16° scope. The results show that DAI increases with the increase of central myopia, among which the DAI between the superior and inferior areas in the vertical retina is larger than the nasal and temporal areas. The DAI between the superior and inferior retinas in group ($-4.0, -2.0$] D, group ($-6.0, -4.0$] D, and group ($-12.0, -6.0$] D were larger than 0.5 D, indicating that visual blur is induced and needs correction. No previous researchers have studied this characteristic in detail, and this study is the first to determine this pattern.

Based on the results, we understand that the RPR shifts to hyperopia along with increasing of central myopia; however, different retinal areas perform differently and asymmetrically. The distribution of RPR is asymmetric, especially in the superior and inferior retinas in the mid or high myopes. Therefore, a regular symmetrical lens cannot perfectly correct the retinal refractive error, and individuals cannot gain perfect visual quality with these lenses in periphery visual field. Thus, we proposed that this asymmetry factor should be considered in any lens to achieve the complete correction of retinal refractive error to improve the visual functions [38] and detection acuity [17] especially for high myopes and those need better periphery vision. The data analysis is mainly focused on spherical equivalent; however, we also have available astigmatism and high-order aberrations that can modify the final optical quality in the periphery. 2D maps of astigmatism and coma are presented as Supplement 1. Through previous research [38] confirmed that peripheral correction may benefit people with impaired central vision regardless of neural mechanisms, but the neural mechanisms are still important to be explored.

The highlight of this study lies in using a unique instrument with high precision and accuracy, allowing the collection of a large amount of data and especially the discovery of the asymmetric distribution of retinal refraction. This finding may be significant for personalized lens design, including spectacles and contact lenses.

Funding. Science Research Foundation of Aier Eye Hospital Group (AF2003D7); National Science and Technology Planning Project (2022YFE0124600); Key Project of Research and Development Plan of Hunan Province (2019SK2051); Agencia Estatal de Investigación (PID2019-105684RB-I00/AEI/10.13039/501100011033).

Disclosures. The authors declare no conflicts of interest.

Data availability. Data of this paper are not publicly available, but it may be obtained from the corresponding author upon reasonable request.

Supplemental document. See [Supplement 1](#) for supporting content.

References

1. A. Klostermann, C. Vater, R. Kredel, and E. J. Hossner, "Perception and Action in Sports. On the Functionality of Foveal and Peripheral Vision," *Front Sports Act Living* **1**(66), 1–17 (2020).
2. J. M. Wood and R. Troutbeck, "Effect of restriction of the binocular visual field on driving performance," *Ophthalmic Physiol Opt* **12**(3), 291–298 (1992).
3. C. Owsley and G. McGwin Jr, "Vision Impairment and Driving," *Surv. Ophthalmol.* **43**(6), 535–550 (1999).
4. B. Wolfe, J. Dobres, R. Rosenholtz, and B. Reimer, "More than the Useful Field: Considering peripheral vision in driving," *Appl Ergon* **65**, 316–325 (2017).
5. C. M. Patino, R. McKean-Cowdin, S. P. Azen, J. C. Allison, F. Choudhury, and R. Varma, and Los Angeles Latino Eye Study Group, "Central and peripheral visual impairment and the risk of falls and falls with injury," *Ophthalmology* **117**(2), 199–206.e1 (2010).
6. L. Tarita-Nistor, E. G. Gonzalez, S. N. Markowitz, L. Lillakas, and M. J. Steinbach, "Increased role of peripheral vision in self-induced motion in patients with age-related macular degeneration," *Invest. Ophthalmol. Vis. Sci.* **49**(7), 3253–3258 (2008).
7. E. L. Smith 3rd and L. F. Hung, "The role of optical defocus in regulating refractive development in infant monkeys," *Vision Res.* **39**(8), 1415–1435 (1999).
8. E. L. Smith, R. Ramamirtham, Y. Qiao-Grider, L.-F. Hung, J. Huang, C.-s. Kee, D. Coats, and E. Paysse, "Effects of Foveal Ablation on Emmetropization and Form-Deprivation Myopia," *Invest. Ophthalmol. Vis. Sci.* **48**(9), 3914–3922 (2007).
9. M. D. Gottlieb, L. A. Fugate-Wentzek, and J. Wallman, "Different visual deprivations produce different ametropias and different eye shapes," *Invest Ophthalmol Vis Sci* **28**(8), 1225 (1987).
10. E. L. Smith, L.-F. Hung, and J. Huang, "Relative peripheral hyperopic defocus alters central refractive development in infant monkeys," *Vision Res.* **49**(19), 2386–2392 (2009).
11. E. L. Smith, L.-F. Hung, J. Huang, and B. Arumugam, "Effects of Local Myopic Defocus on Refractive Development in Monkeys," *Optom Vis Sci.* **90**(11), 1176–1186 (2013).
12. P. Cho, S. W. Cheung, and M. Edwards, "The longitudinal orthokeratology research in children (LORIC) in Hong Kong: a pilot study on refractive changes and myopic control," *Curr Eye Res* **30**(1), 71–80 (2005).
13. P. Cho and S. W. Cheung, "Retardation of myopia in Orthokeratology (ROMIO) study: a 2-year randomized clinical trial," *Invest. Ophthalmol. Visual Sci.* **53**(11), 7077–7085 (2012).
14. P. Sankaridurg, B. Holden, and E. Smith 3rd, "T. Naduvilath, X. Chen, P. L. de la Jara, A. Martinez, J. Kwan, A. Ho, K. Frick, and J. Ge, "Decrease in rate of myopia progression with a contact lens designed to reduce relative peripheral hyperopia: one-year results," *Invest. Ophthalmol. Visual Sci.* **52**(13), 9362–9367 (2011).
15. Y. C. Lee, J. H. Wang, and C. J. Chiu, "Effect of Orthokeratology on myopia progression: twelve-year results of a retrospective cohort study," *BMC Ophthalmol.* **17**(1), 243 (2017).
16. R. S. Anderson, "The selective effect of optical defocus on detection and resolution acuity in peripheral vision," *Curr. Eye Res.* **15**(3), 351–353 (1996).
17. Y. Z. Wang, L. N. Thibos, and A. Bradley, "Effects of Refractive Error on Detection Acuity and Resolution Acuity in Peripheral Vision," *Invest. Ophthalmol. Visual Sci.* **38**(10), 2134 (1997).
18. F. Rempt, J. Hoogerheide, and W. P. Hoogenboom, "Influence of correction of peripheral refractive errors on peripheral static vision," *Ophthalmologica* **173**(2), 128–135 (1976).
19. J. J. Walline, M. K. Walker, D. O. Mutti, L. A. Jones-Jordan, L. T. Sinnott, A. G. Giannoni, K. M. Bickle, K. L. Schulle, A. Nixon, G. E. Pierce, and D. A. Berntsen, "Effect of High Add Power, Medium Add Power, or Single-Vision Contact Lenses on Myopia Progression in Children: The BLINK Randomized Clinical Trial," *JAMA* **324**(6), 571–580 (2020).
20. J. J. Walline, A. G. Giannoni, L. T. Sinnott, M. A. Chandler, J. Huang, D. O. Mutti, L. A. Jones-Jordan, and D. A. Berntsen, "A Randomized Trial of Soft Multifocal Contact Lenses for Myopia Control: Baseline Data and Methods," *Optom. Vis. Sci.* **94**(9), 856–866 (2017).
21. G. R. C. E. Ferree and C. Hardy, "Refraction for the periphery visual field of vision," *Arch. Ophthalmol.* **5**(5), 717–731 (1931).
22. U. L. Osuagwu, M. Suheimat, and D. A. Atchison, "Peripheral aberrations in adult hyperopes, emmetropes and myopes," *Ophthalm. Physiol. Opt.* **37**(2), 151–159 (2017).
23. V. K. Yelagondula, D. S. R. Achanta, S. Panigrahi, S. K. Panthadi, and P. K. Verkicharla, "Asymmetric Peripheral Refraction Profile in Myopes along the Horizontal Meridian," *Optom Vis Sci.* **99**(4), 350–357 (2022).
24. A. Ehsaei, E. A. Mallen, C. M. Chisholm, and I. E. Pacey, "Cross-sectional sample of peripheral refraction in four meridians in myopes and emmetropes," *Invest. Ophthalmol. Visual Sci.* **52**(10), 7574–7585 (2011).
25. X. Chen, P. Sankaridurg, L. Donovan, Z. Lin, L. Li, A. Martinez, B. Holden, and J. Ge, "Characteristics of peripheral refractive errors of myopic and non-myopic Chinese eyes," *Vision Res.* **50**(1), 31–35 (2010).
26. D. A. Atchison, P. N. and K, and L. Schmid, "Peripheral refraction along the horizontal and vertical visual fields in myopia," *Vision Res.* **46**(8-9), 1450–1458 (2006).

27. W. N. Charman and J. A. Jennings, "Longitudinal changes in peripheral refraction with age," *Ophthalm. Physiol. Opt.* **26**(5), 447–455 (2006).
28. B. Jaeken, L. Lundström, and P. Artal, "Fast scanning peripheral wave-front sensor for the human eye," *Opt. Express* **19**(8), 7903 (2011).
29. W. Lan, Z. Lin, Z. Yang, and P. Artal, "Two-dimensional peripheral refraction and retinal image quality in emmetropic children," *Sci. Rep.* **9**(1), 16203 (2019).
30. S. Wang, Z. Lin, X. Xi, Y. Lu, L. Pan, X. Li, P. Artal, W. Lan, and Z. Yang, "Two-dimensional, high-resolution peripheral refraction in adults with isomyopia and anisomyopia," *Invest. Ophthalmol. Visual Sci.* **61**(6), 16 (2020).
31. A. Hartwig, W. N. Charman, and H. Radhakrishnan, "Baseline peripheral refractive error and changes in axial refraction during one year in a young adult population," *J Optom* **9**(1), 32–39 (2016).
32. T. Yamaguchi, K. Ohnuma, K. Konomi, Y. Satake, J. Shimazaki, and K. Negishi, "Peripheral optical quality and myopia progression in children," *Graefes Arch. Clin. Exp. Ophthalmol.* **251**(10), 2451–2461 (2013).
33. D. O. Mutti, L. T. Sinnott, G. L. Mitchell, L. A. Jones-Jordan, M. L. Moeschberger, S. A. Cotter, R. N. Kleinstejn, R. E. Manny, J. D. Twelker, and K. Zadnik, "Relative peripheral refractive error and the risk of onset and progression of myopia in children," *Invest. Ophthalmol. Vis. Sci.* **52**(1), 199–205 (2011).
34. D. A. Atchison, C. E. Jones, K. L. Schmid, N. Pritchard, J. M. Pope, W. E. Strugnell, and R. A. Riley, "Eye shape in emmetropia and myopia," *Invest. Ophthalmol. Vis. Sci.* **45**(10), 3380–3386 (2004).
35. P. K. Verkicharla, K. L. Suheimat, M. Fau - Schmid, D. A. Schmid, K. Fau - Atchison, and D. A. Atchison, "Peripheral Refraction, Peripheral Eye Length, and Retinal Shape in Myopia," *Optom Vis Sci* **93**(9), 1072–1078 (2016).
36. X. Ding, Q. Wang, D. Fau - Huang, J. Huang, Q. Fau - Zhang, J. Zhang, J. Fau - Chang, M. Chang, J. Fau - He, and M. He, "Distribution and heritability of peripheral eye length in Chinese children and adolescents: the Guangzhou Twin Eye Study," *Invest. Ophthalmol. Vis. Sci.* **54**(2), 1048–1053 (2013).
37. D. O. Mutti, J. R. Hayes, G. L. Mitchell, L. A. Jones, M. L. Moeschberger, S. A. Cotter, R. N. Kleinstejn, R. E. Manny, J. D. Twelker, K. Zadnik, and C. S. Group, "Refractive error, axial length, and relative peripheral refractive error before and after the onset of myopia," *Invest. Ophthalmol. Vis. Sci.* **48**(6), 2510–2519 (2007).
38. J. Gustafsson and P. Unsbo, "Eccentric correction for off-axis vision in central visual field loss," *Optometry and Vision Science* **80**(7), 535–541 (2003).